Hindawi
International Journal of Antennas and Propagation
Volume 2023, Article ID 3466400, 6 pages
https://doi.org/10.1155/2023/3466400

Research Article

Design and Measurement of a Vibrating Intrinsic Reverberation Chamber Working in Tuned Mode

Erwei Cheng,[1,2] **Pingping Wang**,[2] **Qian Xu**,[3] **Cui Meng**,[1] **and Rui Jia**[4]

[1]*Department of Engineering Physics, Tsinghua University, Beijing 100084, China*
[2]*National Key Laboratory on Electromagnetic Environment Effects, Army Engineering University Shijiazhuang Campus, Shijiazhuang 050003, China*
[3]*College of Electronic and Information Engineering, Nanjing University of Aeronautics and Astronautics, Nanjing 211106, China*
[4]*63892 Unit of PLA, Luoyang 471000, China*

Correspondence should be addressed to Cui Meng; mengcui@tsinghua.edu.cn

Received 14 July 2022; Revised 14 December 2022; Accepted 24 December 2022; Published 16 January 2023

Academic Editor: Rajkishor Kumar

In this letter, a vibrating intrinsic reverberation chamber (VIRC) working in mode tuning is designed and fabricated; the designed RC is made of a highly electrically conductive silver fabric. A stepper motor is used to tune the cavity surface step by step along its normal direction, and an RC with vibrating wall is realized. The corresponding relationship between the vibrating amplitude and frequency of use is calculated. A test system is developed and the performance of VIRC is experimentally verified. Measurement results show that the measured E-field samples follow a Rician distribution, and the standard deviation of the space E-field is less than 3 dB, which meets the requirements of statistical uniformity tolerance in IEC 61000-4-21.

1. Introduction

Electromagnetic interference may bring threats to the safety and reliability of electronic equipment; thus, reliable electronic devices need to be tested for electromagnetic compatibility (EMC) before being put on the market. An anechoic chamber is a conventional and widely used EMC test environment, and it provides an ideal electromagnetic environment with a single incident direction. Therefore, the EMC test results in such platform may not accurately reflect the actual anti-electromagnetic interference performance of the equipment in a complex electromagnetic environment (e.g., in an aircraft cabin, high Q-factor cavity, *etc* [1]).

The electromagnetic environment in a reverberation chamber (RC) has the characteristics of spatial statistical uniformity, isotropy, and random polarization. Due to the rich multipath reflections, an RC can emulate the electromagnetic environment better than in an anechoic chamber [2, 3], which makes it very suitable for evaluating the immunity of electronic equipment installed in cavity environments [4].

In recent years, a new type of RC called vibrating intrinsic reverberation chamber (VIRC) has emerged. By changing the boundary position of the RC, VIRC can achieve a statistically uniform electromagnetic environment without rotating mechanical stirrers. Compared with conventional RCs, the VIRC has the advantages of large available test space, low cost, and high test efficiency [5, 6]. However, existing VIRCs cannot work in tuned mode [7–15].

One common feature of the models developed in the literature is that the boundary of the RC is random shaking, which leads to the electric field in the RC based on the shaking boundary deformation technology, which is a continuously changing and unstable field. However, some electronic devices require electromagnetic environment irradiation for a period of time to produce interference effects. Therefore, this continuously changing, nonstationary electromagnetic field has limitations when used in the electromagnetic environment effect research of electronic devices, and it may be impossible to find the electromagnetic weaknesses of the type of electronic devices. This limits the application of VIRC in EMC experiments, as some

international standards only accept the mode tuning test of the RC [4].

In this letter, we propose a mode-tuned VIRC method and develop a test system for measurements in RC. The organization of the article is as follows. Section 2 describes the VIRC model construction method and vibrating amplitude calculation method. Section 3 describes the developed VIRC test system. Section 4 verifies the effectiveness of the test system experimentally, and the consistency between the test results and the theory can be observed.

2. VIRC Model Based on Surface Vibration

2.1. Construction of the Cavity Surface Vibration Model. VIRC is achieved by driving a stepper motor connected to the center point of the surface back and forth along its normal direction. Therefore, a VIRC can be approximately modeled as a combination of a rectangular cavity and a quadrangular pyramid, where the height of the quadrangular pyramid is the amplitude of the vibration of VIRC. The synthesis of a series of quadrangular pyramid and rectangular cavities with different heights is the discrete form of VIRC in the time domain. The VIRC model established by this method is shown in Figure 1.

2.2. Calculation Method of Vibration Amplitude of a Cavity Surface. According to Weyl's law, the number of resonance modes in a rectangular cavity can be given in the form of wavelength and volume, which is approximately

$$N_s(f) = \frac{8\pi V}{3\lambda^3}. \tag{1}$$

The variation of the number of modes can be linked to the volume variation as follows:

$$\Delta N_s = \frac{8\pi}{3\lambda^3}\Delta V. \tag{2}$$

When $\Delta N_s = 1$ which means the resonance mode is shifted to the next mode, the perturbation of the volume can be obtained as follows:

$$\Delta V \approx \frac{3\lambda^3}{8\pi}. \tag{3}$$

The perturbation of the VIRC volume is equal to the increase or decrease of the volume of the quadrangular pyramid. The perturbation of the volume of a quadrangular pyramid can be obtained as follows:

$$\Delta V = \frac{1}{3}\left(S_{\text{up}} + \sqrt{S_{\text{up}}S_{\text{lo}}} + S_{\text{lo}}\right)\Delta h, \tag{4}$$

where S_{up} and S_{lo} represent the area of the upper and lower surface of the quadrangular pyramid, respectively, and Δh represents the perturbed height of the quadrangular pyramid.

Since each deformation of the RC is required to be able to change the distribution structure significantly of the electromagnetic field inside the cavity, the vibration step of the RC is equal to the change of the height of the quadrangle. We substitute formula (4) into formula (3) to obtain the step amplitude of VIRC:

$$\Delta h = \frac{9\lambda^3}{8\pi\left(S_{\text{up}} + \sqrt{S_{\text{up}}S_{\text{lo}}} + S_{\text{lo}}\right)}. \tag{5}$$

The paddle of a mechanically stirred RC needs to reside in at least 12 positions to obtain good statistical space E-fields [2]. Accordingly, the number of vibration step of VIRC is required to be at least 12. Thus, the vibration amplitude of the VIRC can be determined as follows:

$$l \geq 12\Delta h = \frac{27\lambda^3}{2\pi\left(S_{\text{up}} + \sqrt{S_{\text{up}}S_{\text{lo}}} + S_{\text{lo}}\right)}. \tag{6}$$

3. Fabrication of VIRC

The VIRC cavity was made of a silver fiber shielding cloth, the shielding effectiveness of which is about 50 dB. A rectangular cavity with dimensions of 2.5 m × 1.8 m × 1.5 m was built with the cloth, and its eight vertices are fixed on a bigger meal frame. The bottom of VIRC is close to the ground. All surfaces of VIRC except the bottom can be moved by motor traction. A hole with a size of 1 m × 0.8 m was opened on one surface of the VIRC, through which the test equipment could be put into the VIRC. We use a silver fiber cloth slightly larger than the area to cover the hole to prevent electromagnetic leakage. A stepping motor was used to drive a surface of the VIRC to reciprocate along its normal direction. The proto type of the VIRC is shown in Figure 2.

An automatic test system is depicted in Figure 3 using a signal generator, a power amplifier, a power meter, a spectrum analyzer, *etc*. The signal generator was used to generate the required continuous wave signal, which was amplified by a wideband power amplifier and feed to the transmitting antenna in the VIRC. The power meter was used to monitor the forward and reverse power of the system. The reference-receiving antenna was placed inside the working area of the RC, and the received signal was monitored by the spectrum analyzer through a coaxial cable. The schematic diagram of the test system is shown in Figure 3. The actual test picture is shown in Figure 4.

4. Evaluation of Space E-Field Characteristics in VIRC

4.1. Characteristics of the E-Field inside the VIRC. VIRC operates in stirring mode during E-field characteristic testing. The E-field meter was placed in the working area of the RC to test the E-field. A set of E-field data was recorded every 3 s, and a total of 500 sets of test data were recorded. The cumulative probability density functions of E-field samples at two frequencies, 200 MHz and 600 MHz, were measured, and the test results are shown in Figure 5.

The solid line in Figure 5 represents the theoretical Rician distribution function, and the dotted line represents the cumulative probability distribution function of the

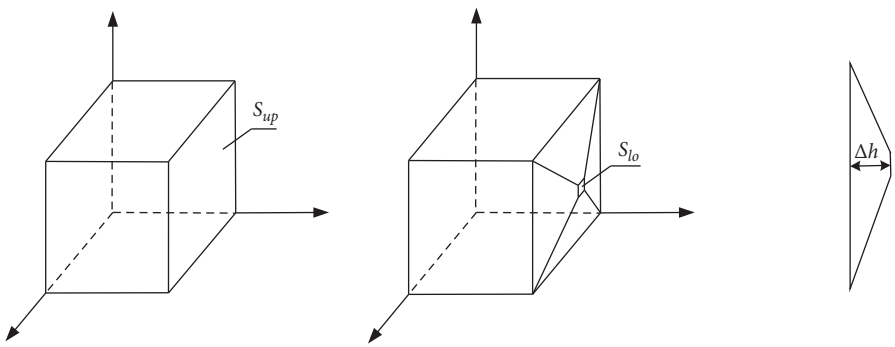

Figure 1: Schematic diagram of the VIRC model.

Figure 2: The proto type of the VIRC.

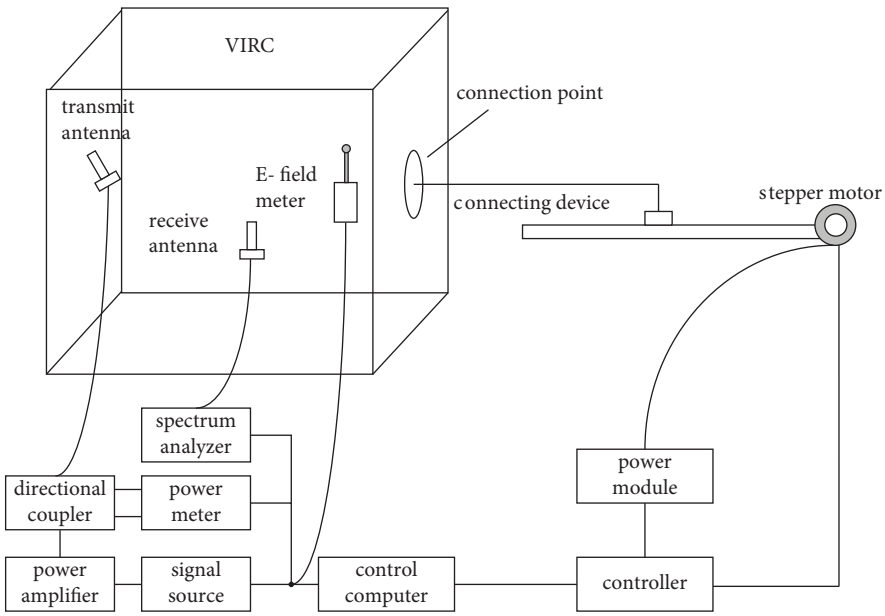

Figure 3: Diagram of the test system.

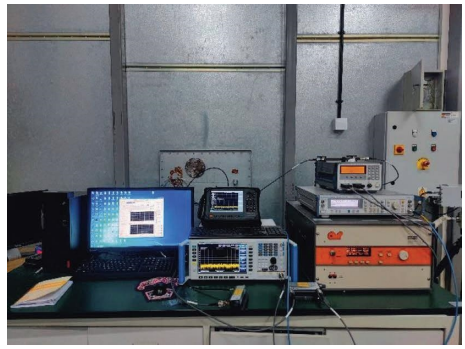

Figure 4: The figure of measurement.

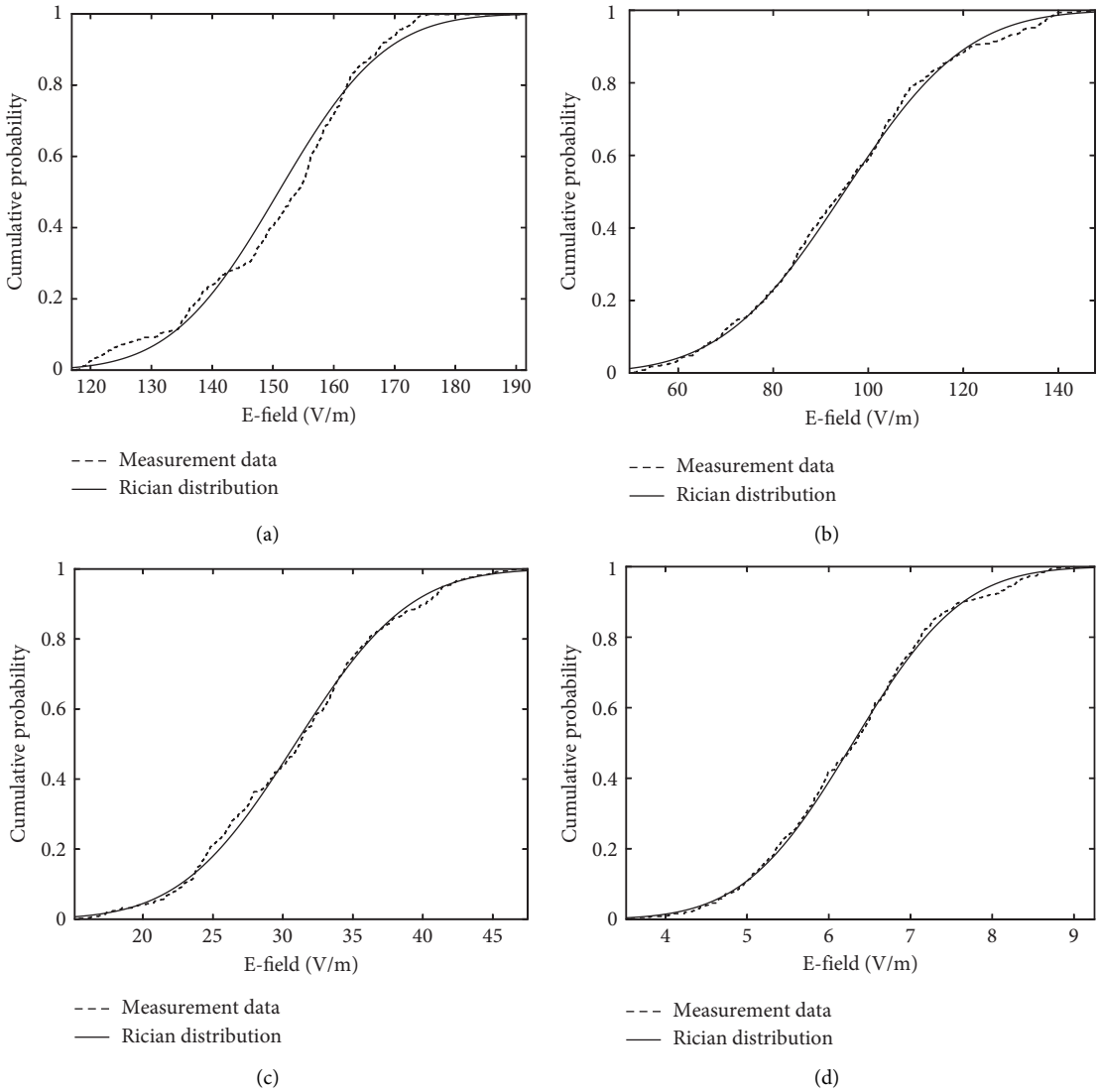

Figure 5: Probability distribution function of E-field in the RC. (a) $f = 200$ MHz, (b) $f = 600$ MHz, (c) $f = 1000$ MHz, and (d) $f = 10$ GHz.

actual test data. It can be seen that at 200 MHz, there is a significant deviation between the measured data and the theoretical Rician distribution function, which reflects the poor statistical characteristics of the E-field inside the RC. With the increase of frequency, the measured data and the theoretical Rician distribution function tend to be consistent.

One of the characteristics of the reverberation chamber is that the distribution function has a large deviation from the theory at a lower frequency. When the frequency is

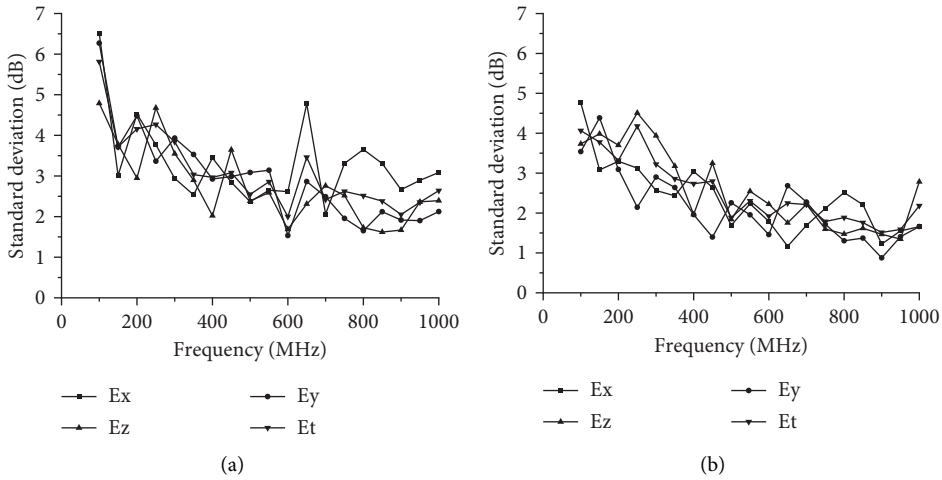

Figure 6: The statistical uniformity of the spatial e-field inside the VIRC. (a) Amplitude 20 cm and (b) Amplitude 40 cm.

Table 1: Comparison with traditional methods.

Items	New method	Traditional method
Test system	Relatively complex	Simple
Statistical uniformity of spatial electric field	Easy access	Not easy to obtain, and the deformation amplitude and other parameters need to be adjusted many times
Working mode	Mode-tuned	Mode-stirred
Application range	Suitable for EMI testing of all types of electronic equipment	Only suitable for EMI test of energy sensitive electronic equipment

higher, the consistency between the probability distribution function and the theoretical analysis will be better. For the VIRC studied in this paper, 200 MHz is a lower frequency case, and the consistency of the probability density function is not good at this time. With the increase of frequency, when the frequency is 600 MHz, 1000 MHz, 10 GHz, theoretically, the probability density function of the reverberation chamber should become better. In fact, the measurement data also support this view. Although there is not much measurement data in the higher frequency range, it could be expected that the electric field distribution characteristics of the reverberation chamber in the wider frequency range are still good.

4.2. E-Field Uniformity inside the VIRC. In the uniformity test, the VIRC is in tuning mode. According to formula (6), the vibration amplitude can be chosen to be 40 cm. In order to study the influence of vibration amplitude on uniformity, the vibration amplitude of 20 cm was also measured, and the results are shown in Figure 6.

In Figure 6, *Ex*, *Ey*, and *Ez* represent the standard deviation of the *x*, *y*, and *z* components of the maximum E-field, respectively, and *Et* represents the standard deviation of the total E-field intensity. It can be seen that the standard deviation of the E-field shows a decreasing trend with the increase of frequency, which indicates that the uniformity of the VIRC is improving. The vibration amplitude has a significant effect on the E-field uniformity, when the vibration amplitude reaches 40 cm, the standard deviation of all frequencies in the range of 500 MHz–1000 MHz is less than 3 dB, which meets the requirements of IEC 61000-4-21 for the uniformity of the RC.

4.3. Comparison with Traditional Methods. Table 1 shows the comparison between the new method and the traditional method. From the perspective of system composition, the new method is slightly more complex than the traditional method. The traditional method is easy to realize by pulling the corner or edge of the reverberation chamber for vibration or random deformation. The new method requires at least one guide rail, one or more surfaces of the traction reverberation chamber are deformed, and the system is relatively complex.

Traditional methods are difficult to obtain the statistical uniformity of spatial electric field, because the vibration amplitude needs to be explored, and it may require multiple adjustments to the reverberation chamber vibration method to achieve the acquisition of the spatial statistical uniformity of the electromagnetic environment. Using the new method to make VIRC, the deformation amplitude has clear theoretical guidance, and it can be expected to obtain a good RC environment easily.

In terms of the internal electric field distribution characteristics, VIRC made by traditional methods can only work in mode stirred, so the internal field distribution is unstable, which is an electromagnetic field that changes with time. Therefore, it can only be used for the EMI test of energy sensitive electronic equipment. The VIRC made by the new

method can work in tuned mode, with a wider range of applications, and can be used for EMI testing of all types of electronic equipment.

5. Conclusion

In this letter, a method for designing surface vibration VIRCs that can operate in mode-tuning mode has been proposed. The proposed VIRC is made of a silver fiber shielding cloth, and a stepping motor is used to drive the cavity surface to move in the normal direction. The linear stepping mode of the motor makes it possible for the VIRC to work in mode tuning. The calculation method of the vibration amplitude of VIRC is proposed, and the performance evaluation test of the developed VIRC is carried out. The results show that the E-field inside the VIRC obeys the theoretical Rician distribution. When the vibration amplitude reaches 40 cm, the standard deviation of the E-field is less than 3 dB, which meets the requirements of EMC on the uniformity of the platform. Measurements confirm that a VIRC with good statistical properties can be realized by applying the surface vibration technique.

Data Availability

The data used to support the findings of this study are currently under embargo while the research findings are commercialized. Requests for data, [6/12 months] after publication of this article, will be considered by the corresponding author.

Conflicts of Interest

The authors declare that they have no conflicts of interest.

Acknowledgments

This work was supported by the National Natural Science Foundation of China under Grant no. 51677191.

References

[1] R. S. Langley, "A reciprocity approach for computing the response of wiring systems to diffuse electromagnetic fields," *IEEE Transactions on Electromagnetic Compatibility*, vol. 52, no. 4, pp. 1041–1055, 2010.

[2] IEC, *IEC 61000-4-21 Electromagnetic Compatibility (EMC), Part 4-21: Testing and Measurement Techniques-Reverberation Chamber Test Methods*, International Electrotechnical Commission, Geneva, Switzerland, 2011.

[3] A. Reis, F. Sarrazin, E. Richalot et al., "Radar cross section pattern measurements in a mode-stirred reverberation chamber: theory and experiments," *IEEE Transactions on Antennas and Propagation*, vol. 69, no. 9, pp. 5942–5952, 2021.

[4] RTCA DO-160G, *Environmental Conditions and Test Procedures for Airborne Equipment*, Radio Technical Commission, Washington, D.C. USA, 2010.

[5] R. Serra and F. Leferink, "Optimizing the stirring strategy for the vibrating intrinsic reverberation chamber," in *Proceedings of the 9th International Symposium on EMC and 20th International Wroclaw Symposium on Electromagnetic Compatibility*, pp. 457–462, IEEE, Wroclaw, Poland, September 2010.

[6] M. Hara, Y. Takahashi, and R. Vogt-Ardatjew, "Statistical analysis for reverberation chamber with flexible shaking walls with various amplitudes," in *Proceedings of the 2018 International Symposium on Electromagnetic Compatibility*, pp. 694–698, IEEE, Amsterdam, Netherlands, October 2018.

[7] J. Skrzypczynski, "On shielding effectiveness measurements using dual Vibrating Intrinsic Reverberation Chamber," in *Proceedings of the International Conference on Software, Telecommunications and Computer Networks*, pp. 112–116, Split, Croatia, September 2010.

[8] V. Gkatsi, R. Vogt-Ardatjew, H. Schipper, and F. Leferink, "Board level shielding effectiveness measurements using the dual VIRC," in *Proceedings of the 2021 Asia-Pacific International Symposium on Electromagnetic Compatibility (APEMC)*, pp. 1–4, Nusa Dua - Bali, Indonesia, September 2021.

[9] M. Hara, T. Yoshikai, Y. Takahashi, R. Vogt-Ardatjew, and F. Leferink, "Numerical analysis of vibrating intrinsic reverberation chamber between various shielding effectiveness measurement techniques," in *Proceedings of the 2020 International Symposium on Electromagnetic Compatibility - EMC EUROPE*, pp. 1–6, Rome, Italy, September 2020.

[10] J. Geerarts and R. Serra, "Wave Chaos in the vibrating intrinsic reverberation chamber," in *Proceedings of the 2021 IEEE International Joint EMC/SI/PI and EMC Europe Symposium*, Raleigh, NC, USA, August 2021.

[11] D. Izzo, R. Vogt-Ardatjew, and F. Leferink, "Experimental Observations of the Minimum Dwell time for Radiated immunity tests in a vibrating intrinsic reverberation chamber," in *Proceedings of the 2021 Asia-Pacific International Symposium on Electromagnetic Compatibility (APEMC)*, pp. 1–4, Nusa Dua - Bali, Indonesia, September 2021.

[12] D. Izzo, R. Vogt-Ardatjew, and F. Leferink, "Considerations on the Dwell time for a vibrating intrinsic reverberation chamber," in *Proceedings of the 2021 IEEE International Joint EMC/SI/PI and EMC Europe Symposium*, pp. 355–360, Raleigh, NC, USA, August 2021.

[13] D. Izzo, A. Rommel, M. Aidam, R. Vogt-Ardatjew, and F. Leferink, "A Cosed-Loop Calibration method for the vibrating intrinsic reverberation chamber," in *Proceedings of the 2020 International Symposium on Electromagnetic Compatibility - EMC EUROPE*, pp. 1–6, Rome, Italy, September 2020.

[14] D. Izzo, A. Rommel, R. Vogt-Ardatjew, and F. Leferink, "Validation and use of a vibrating intrinsic reverberation chamber for radiated immunity tests," in *Proceedings of the 2020 IEEE International Symposium on Electromagnetic Compatibility & Signal/Power Integrity (EMCSI)*, pp. 56–60, Reno, NV, USA, August 2020.

[15] G. Andrieu, N. Meddeb, C. Jullien, and N. Ticaud, "Complete framework for frequency and time-domain performance assessment of vibrating intrinsic reverberation chambers," *IEEE Transactions on Electromagnetic Compatibility*, vol. 62, no. 5, pp. 1911–1920, Oct, 2020.